

# Momentum creation by vortices in $^3\text{He}$ experiments as a model of primordial baryogenesis.

T.D.C. Bevan<sup>1</sup>, A.J. Manninen<sup>1,2</sup>, J.B. Cook<sup>1</sup>, J.R. Hook<sup>1</sup>, H.E. Hall<sup>1</sup>, T. Vachaspati<sup>3</sup> and G.E. Volovik<sup>4,5</sup>

An important problem in cosmology is why the universe contains so much more matter than antimatter. Such an imbalance can result from processes in which baryon number is not conserved. These may have occurred during the electroweak phase transition in the early universe when elementary particles first acquired mass [1–3]. The standard model of particle physics has been thoroughly tested in terrestrial accelerator experiments where relatively low energies are involved and perturbation theory can be used to make predictions. But these experiments and calculations are unable to probe the processes expected to occur during the electroweak phase transition, which involve large departures from the vacuum state. It is worthwhile therefore to investigate systems where similar processes can be studied experimentally. Superfluid  $^3\text{He}$  has many similarities to the standard electroweak model [4]. The analogue of cosmic string production has already been demonstrated in condensed matter [5–9]. Here we explain how recent  $^3\text{He}$  experiments at Manchester demonstrate the creation of excitation momentum (momentogenesis) by quantized vortices,

---

<sup>1</sup> Schuster Laboratory, University of Manchester, Manchester, M13 9PL, UK

<sup>2</sup> Now at Physics Dept., University of Jyväskylä, P.O.Box35, 40351 Jyväskylä, Finland

<sup>3</sup> Physics Department, Case Western Reserve University, Cleveland, OH 44106, USA

<sup>4</sup> Low Temperature Laboratory, Helsinki University of Technology, 02150 Espoo, Finland

<sup>5</sup> Landau Institute for Theoretical Physics, 117334 Moscow, Russia.

### **a process analogous to baryogenesis within cosmic strings.**

To explain the creation of matter in the early universe we begin by recalling the relationship  $E^2 = m_0^2 c^4 + p^2 c^2$  between energy  $E$  and momentum  $p$  for relativistic particles with rest mass  $m_0$ . Dirac realised that the square root of this equation  $E = \pm \sqrt{m_0^2 c^4 + p^2 c^2}$  produced particles with both positive and negative energy. This led to his famous picture of the vacuum state (the state with no real particles) as one in which all the negative energy states are full and all the positive energy states are empty. A real particle is then created as shown in Fig. 1(a) by excitation of a particle from the “Dirac sea” of negative energy states to a positive energy state. Such processes however create matter and antimatter in equal amounts since the appearance of a hole in the negative energy states is interpreted as the simultaneous creation of an antiparticle.

The net creation of matter in the form of baryons such as protons and neutrons requires processes in which antiparticles are not simultaneously created and thus baryon number is not conserved. In the standard model the baryon number is classically conserved but can be violated by quantum mechanical effects known generically as “chiral anomalies”. The process leading to matter creation is called “spectral flow” and can be pictured as a process in which particles flow from negative energies to positive energies under the influence of an external force. In this way real observable positive energy particles can appear without simultaneous creation of antiparticles. Fig. 1(b) illustrates a simple example of spectral flow occurring for massless particles with electric charge  $q$  (in units of the charge of the electron) moving in a magnetic field. The application of an electric field  $\mathbf{E}$  leads to the production of particles from the vacuum at the rate

$$\dot{n} = \partial_\mu j^\mu = \frac{q^2}{4\pi^2} \mathbf{E} \cdot \mathbf{B} \tag{1}$$

per unit volume; factors of  $(e/\hbar)$  have been absorbed in the definition of the electric and magnetic fields. This is an anomaly equation for the production of particles from the vacuum of the type found by Adler [10] and by Bell and Jackiw [11] in the context of neutral pion decay. We see that for particle creation it is necessary to have an asymmetric branch of the

dispersion relation  $E(p)$  which crosses the axis from negative to positive energy. We call such a branch a zero mode branch; a spectrum of this type was first found for vortex core excitations in a superconductor [12].

Similar zero mode branches exist on a cosmic electroweak string (also known as a Z-string), which is a structure of the Higgs field that may have been produced during the electroweak phase transition. The Higgs field gives the particles mass outside the string core. This field vanishes on the string axis and the fermions (quarks and leptons) living in the core of the string behave like massless one-dimensional particles. Spectral flow on a Z-string leading to production of baryons from the vacuum with conservation of electric charge is illustrated in Fig. 1(c). Motion of the string across a background electromagnetic field [13] or the de-linking of two linked loops [14,15] provides a mechanism for cosmological baryogenesis [16] and could lead to the presence of antimatter in cosmic rays [17].

We should point out that baryon number violation is only one ingredient in a cosmological baryogenesis scenario. The other ingredients are that the system has to be out of thermal equilibrium, and charge (C) and charge-parity conjugation (CP) symmetries should be violated; these conditions are known as the ‘‘Sakharov conditions’’ for cosmological baryogenesis [18]. In condensed matter the analogous symmetry breaking is provided by rotation (for  $^3\text{He}$ ) or a magnetic field (for superconductors), and disequilibrium is provided by the motion of vortex lines. We shall see that excitation momentum is the analogue of baryon number.

The superfluidity of  $^3\text{He}$  is due to the formation of bound pairs of  $^3\text{He}$  atoms known as Cooper pairs. There are two main superfluid phases, A and B, which have different Cooper pair wave functions. At the lowest temperature the superfluid vacuum state is obtained in which all the atoms are Cooper paired. By analogy with the Dirac picture of the vacuum (Fig. 1(a)) the Cooper-paired atoms are seen as filling all the negative energy states and are separated from the world of normal particles by the Cooper pair binding energy. The Cooper pair wave function (usually called the order parameter) which is responsible for this energy gap is thus analogous to the Higgs field in electroweak theory since it is the finite

particle mass produced by the Higgs field that results in the energy gap in electroweak theory between the negative and positive energy states in Fig. 1(a). At higher temperatures in  $^3\text{He}$  some atoms are excited from the ground state by the breaking of Cooper pairs and these normal (non-superfluid) excitations interact with the order parameter in a way that is similar to the interaction of the standard model particles with the electroweak gauge and Higgs fields. Thus the behaviour of leptons and quarks on fixed gauge and Higgs field backgrounds can be modelled by the behaviour of  $^3\text{He}$  excitations on fixed order parameter backgrounds such as quantized vortices. In  $^3\text{He}$  a zero mode branch exists for particles in the core of quantized vortices (Fig. 2(a)). A physically important charge in  $^3\text{He-A}$ ,  $^3\text{He-B}$  and superconductors which, like baryonic charge in the standard model, is not conserved due to the anomaly, is excitation momentum. Spectral flow along the zero mode branch leads to an additional “lift” force on a moving vortex (Fig. 2(b), the analogue of Fig. 1(c)).

This is most easily seen for the doubly quantized continuous vortex (winding number  $N = 2$ ) in the A-phase of superfluid  $^3\text{He}$ , which is the closest analogue of a Z-string. The Cooper pairs in  $^3\text{He-A}$  have angular momentum  $\hbar$  and locally all the pairs have this angular momentum aligned along a direction  $\hat{\mathbf{I}}$ . The  $N = 2$  vortex is characterized by a continuous distribution of the order parameter vector  $\hat{\mathbf{I}}$  as shown in Fig. 2(c). The time and space dependent  $\hat{\mathbf{I}}$  vector associated with the motion of the vortex produces a force on the excitations equivalent to that of an “electric field”  $\mathbf{E} = k_F \partial_t \hat{\mathbf{I}}$  and a “magnetic field”  $\mathbf{B} = k_F \nabla \times \hat{\mathbf{I}}$  acting on particles of unit charge, where  $k_F = p_F/\hbar$  and  $p_F$  is the Fermi momentum. Equation (1) can then be applied to calculate the rate at which left-handed quasiparticles and right-handed quasiholes are created by spectral flow. Since both types of excitation have momentum  $p_F \hat{\mathbf{I}}$ , excitation momentum is created at a rate

$$\partial_t \mathbf{P} = \frac{1}{2\pi^2} \int d^3r p_F \hat{\mathbf{I}} (\mathbf{E} \cdot \mathbf{B}) . \quad (2)$$

However, total linear momentum must be conserved. Therefore Eq. (2) means that, in the presence of a time-dependent texture, momentum is transferred from the superfluid ground state (analogue of vacuum) to the heat bath of excitations forming the normal component

(analogue of matter).

Integration of the anomalous momentum transfer in Eq.(2) over the cross-section of the moving vortex gives the loss of linear momentum and thus the additional force per unit length acting on the vortex due to spectral flow:

$$\mathbf{F}_{\text{sf}} = \partial_t \mathbf{P} = \pi \hbar N C_0 \hat{\mathbf{z}} \times (\mathbf{v}_n - \mathbf{v}_L) \quad . \quad (3)$$

Here  $\hat{\mathbf{z}}$  is the direction of the vortex,  $C_0 = k_F^3/3\pi^2$ ,  $\mathbf{v}_L$  is the velocity of the vortex line,  $\mathbf{v}_n$  is the heat bath velocity, and  $N$  is the winding number of the vortex.

The insets to Fig. 3(a) show how the force on a vortex is measured experimentally. A uniform array of vortices is produced by rotating the whole cryostat, and oscillatory superflow perpendicular to the rotation axis is produced by a vibrating diaphragm, while the normal fluid (thermal excitations) is clamped by viscosity. The velocity  $\mathbf{v}_L$  of the vortex array is determined by the overall balance of forces acting on the vortices, conventionally written as [19,20]

$$n_s \pi \hbar N \left[ \hat{\mathbf{z}} \times (\mathbf{v}_L - \mathbf{v}_s) + d_{\perp} \hat{\mathbf{z}} \times (\mathbf{v}_n - \mathbf{v}_L) + d_{\parallel} (\mathbf{v}_n - \mathbf{v}_L) \right] = 0 \quad , \quad (4)$$

where  $n_s(T)$  and  $\mathbf{v}_s$  are the density and velocity of the superfluid component. The first term is the Magnus force, which appears when the vortex moves with respect to the superfluid and the terms with  $(\mathbf{v}_n - \mathbf{v}_L)$  represent the nondissipative transverse and frictional longitudinal forces, proportional to dimensionless parameters  $d_{\perp}$  and  $d_{\parallel}$  respectively, which appear if the vortex moves with respect to the normal fluid. The diaphragm has to provide a force equal and opposite to the Magnus force to drive the superfluid. Measurement of the damping of the diaphragm resonance and of the coupling between the two orthogonal modes illustrated in Fig. 3(a) enables both  $d_{\perp}$  and  $d_{\parallel}$  to be deduced.

For the A-phase the spectral flow force in Eq. (3) combines with the Iordanskii force [19] to give  $d_{\perp} \approx (C_0 - n_n)/n_s$ , where  $n_n(T) = n - n_s(T)$  is the density of the normal component, with  $n$  the total density. Since  $C_0 \approx n$ , one has  $d_{\perp} \approx 1$ . Our  ${}^3\text{He-A}$  experiments made at 29.3bar and  $T > 0.82T_c$  are consistent with this within experimental uncertainty: we find that  $|1 - d_{\perp}| < 0.005$  [21].

Any Fermi superfluid becomes similar to the A-phase in the vicinity of the vortex core. However, in  ${}^3\text{He-B}$  the spacing  $\hbar\omega_0$  between bound states on the anomalous branch in Fig. 2(a) becomes larger than the lifetime broadening  $\hbar\tau^{-1}$  at low  $T$  [19]. There should thus be a transition from full spectral flow as  $T \rightarrow T_c$  to totally suppressed spectral flow as  $T \rightarrow 0$ , a further aspect of the theory which can be tested experimentally. The interpolation formula as a function of the relaxation parameter  $\omega_0\tau$  and the spectral flow parameter  $C_0 \approx n$  [19,22] can be written in the form

$$d_{\parallel} - j(1 - d_{\perp}) = \frac{1}{\alpha + j(1 - \alpha')} = \frac{n}{n_s} \frac{\omega_0\tau}{1 + j\omega_0\tau} \tanh \frac{\Delta(T)}{2k_B T} , \quad (5)$$

where  $j = \sqrt{-1}$  and the  $\alpha$  parameters are what are directly measured experimentally [20]. The experimental results are compared with Eq. (5) in Fig. 3. The agreement is excellent in view of the approximations in the theory.

Our results thus show that the chiral anomaly is relevant for the interaction of condensed matter vortices (analogue of strings) with fermionic excitations (analogue of quarks and leptons); this gives a firmer footing to chiral anomaly calculations for baryogenesis on non-trivial backgrounds of the Higgs field such as cosmic strings. Superfluid  ${}^3\text{He}$  is the most complex field theoretic system available in the laboratory, and is therefore the closest experimental analogue of the field theoretic foundations of the physics of the early universe. It is characteristic of non-linear theories that experiment often reveals qualitatively new phenomena that would be hard to find by contemplation of the equations alone. We may therefore hope that imaginative experiments on superfluid  ${}^3\text{He}$  will generate new ideas in cosmology.

## REFERENCES

- [1] A.D. Dolgov *Nongut baryogenesis* Phys. Rept., **222**, 309–386 (1992).
- [2] N.Turok *Electroweak baryogenesis* in Formation and interaction of topological defects, eds. A.C.Davis, R.Brandenberger (Plenum Press, New York,London),1995, pp. 283–301.
- [3] A. Vilenkin and E.P.S. Shellard, *Cosmic Strings and Other Topological Defects* (Cambridge University Press, 1994); M.B.Hindmarsh and T.W.B. Kibble *Cosmic Strings* Rep. Prog. Phys. **58**, 477–562 (1995).
- [4] G.E. Volovik and T. Vachaspati *Aspects of  $^3\text{He}$  and the standard electroweak model* Int. J. Mod. Phys. **B 10**, 471–521 (1996).
- [5] W.H. Zurek *Cosmological experiments in superfluid helium* Nature **317**, 505–508 (1985).
- [6] I. Chuang, R. Durrer, N. Turok, and B. Yurke *Cosmology in the laboratory: defect dynamics in liquid crystals* Science **251**, 1336–1342 (1991); M.J. Bowick, L. Chander, E.A. Schiff, and A.M. Srivastava *The cosmological Kibble mechanism in the laboratory: string formation in liquid crystals* Science **263**, 943–945 (1994).
- [7] P.C. Hendry, N.S. Lawson, R.A.M. Lee, P.V.E. McClintock, and C.D.H. Williams *Generation of defects in superfluid  $^4\text{He}$  as an analogue of the formation of cosmic strings* Nature **368**, 315–317 (1994).
- [8] V.M.H.Ruutu, V.B.Eltsov, A.J.Gill, T.W.B Kibble, M.Krusius, Yu.G.Makhlin, B.Placais, G.E.Volovik and Wen Xu *Vortex formation in neutron irradiated  $^3\text{He}$  as an analogue of cosmological defect formation* Nature **382**, 334–336 (1996).
- [9] C.Bäuerle, Yu.M.Bunkov, S.N.Fisher, H.Godfrin, G.R.Pickett *Laboratory simulation of cosmic string formation in the early Universe using superfluid  $^3\text{He}$*  Nature **382**, 332–334 (1996).
- [10] S. Adler *Axial-vector vertex in spinor electrodynamics* Phys. Rev. **177**, 2426–2438

- (1969).
- [11] J.S.Bell and R.Jackiw *A PCAC puzzle:  $\pi^0 \rightarrow \gamma\gamma$  in the  $\sigma$ -model* Nuovo Cim. Ser. 10 **60A**, 47–61 (1969).
- [12] C. Caroli, P.G. de Gennes, and J. Matricon *Bound fermion states on a vortex line in a type II superconductor* Phys. Lett., **9**, 307–309 (1964).
- [13] E. Witten *Superconducting strings* Nucl. Phys. **B249**, 557–592 (1985).
- [14] T. Vachaspati and G.B. Field *Electroweak string configurations with baryon number* Phys. Rev. Lett. **73**, 373–376 (1994); **74**, 1258(E) (1995).
- [15] J. Garriga and T. Vachaspati *Zero modes on linked strings* Nucl. Phys. **B438**, 161–181 (1995).
- [16] M. Barriola *Electroweak strings produce baryons* Phys. Rev. **D51**, 300-304 (1995).
- [17] G.D. Starkman and T. Vachaspati *Galactic cosmic strings as sources of primary antiprotons* Phys. Rev. **D53**, 6711–6714 (1996).
- [18] A. Sakharov *Violation of CP invariance, C asymmetry, and baryon asymmetry of the Universe* Pisma ZhETF **5**, 32–35 (1967); [JETP Lett. **5**, 24–27 (1967)].
- [19] N.B. Kopnin, G.E. Volovik, and Ü. Parts *Spectral flow in vortex dynamics of  $^3\text{He-B}$  and superconductors* Europhys. Lett. **32**, 651–656 (1995).
- [20] T.D.C. Bevan, A.J. Manninen, J.B. Cook, A.J. Armstrong, J.R. Hook, and H.E. Hall *Vortex mutual friction in rotating superfluid  $^3\text{He-B}$*  Phys. Rev. Lett. **74**, 750–753 (1995) (correction **74**, 3092).
- [21] A.J.Manninen, T.D.C.Bevan, J.B.Cook, H.Alles, J.R.Hook and H.E.Hall *Vortex mutual friction, orbital inertia and history dependent textures in rotating superfluid  $^3\text{He-A}$*  Phys. Rev. Lett. **77**, 5086–5089 (1996).



- [22] M. Stone *Spectral flow, Magnus force and mutual friction via the geometric optics limit of Andreev reflection* Phys. Rev. **B 54**, 13222–13229 (1996).
- [23] Ü. Parts, J.M. Karimäki, J.H. Koivuniemi, M. Krusius, V.M.H. Ruutu, E.V. Thuneberg, and G.E. Volovik *Phase diagram of vortices in superfluid  $^3\text{He-A}$*  Phys. Rev. Lett. **75**, 3320–3323 (1995).

ACKNOWLEDGEMENTS. The Manchester authors thank Mike Birse for advice on field theory and EPSRC for financial support. TV was partially supported by the US Department of Energy.

CORRESPONDENCE to Henry.Hall@man.ac.uk

## FIGURE CAPTIONS

Fig. 1: (a) Particles and antiparticles in the Dirac picture; the thick line shows occupied negative energy states. Promotion of a particle from negative energy to positive energy creates a particle-antiparticle pair from the vacuum.

(b) Spectrum of massless right-handed particles in a magnetic field  $\mathbf{B}$  along  $z$ ; the thick lines show the occupied negative-energy states. The right-handed chirality of the particles means that their spin is aligned with their linear momentum. Motion of the particles in the plane perpendicular to  $\mathbf{B}$  is quantized into the Landau levels shown. The free motion is thus effectively reduced to one-dimensional motion along  $\mathbf{B}$  with momentum  $p_z$ . Because of the chirality of the particles the lowest ( $n = 0$ ) Landau level, for which  $E = cp_z$ , is asymmetric: it crosses zero only in one direction. If we now apply an electric field  $\mathbf{E}$  along  $z$ , particles are pushed from negative to positive energy levels according to the equation of motion  $\dot{p}_z = qE$ , and the whole Dirac sea moves up, creating particles and electric charge from the vacuum. This motion of the particles along the “anomalous” branch of the spectrum is called spectral flow. The rate of particle production is proportional to the density of states at the Landau level, which is  $\propto q|\mathbf{B}|$ , so that the rate of production of particles from the vacuum is  $\propto q^2\mathbf{E} \cdot \mathbf{B}$ .

(c) Anomalous branches of the spectrum of u-quarks ( $q = +2/3$ ) and d-quarks ( $q = -1/3$ ) in the core of a Z-string. There are anomalous branches for electrons ( $q = -1$ ) and neutrinos ( $q = 0$ ) also. The neutrino and u-quark propagate in one direction along the string while the electron and d-quark propagate in the opposite direction. For every electron produced, two u-quarks and one d-quark are created so that there is no net production of electric charge but the baryon number  $B$  increases by one (2 u-quarks + 1 d-quark  $\equiv$  1 proton = 1 baryon).

Fig. 2: (a) Spectrum of particles in the core of vortices in  $^3\text{He}$  and superconductors; filled circles show occupied states. The only difference from the Z-string is that the anomalous branch,  $E_0(p_z, L_z) = -L_z\hbar\omega_0(p_z)$ , of the spectrum crosses zero as a function of the discrete angular momentum  $\hbar L_z$ , where  $L_z$  is a half-odd integer. Typically the interlevel distance

$\hbar\omega_0$  is very small compared to the characteristic energy scales in superconductors and Fermi superfluids, and can be comparable to the level width  $\hbar/\tau$  resulting from the scattering of core excitations by free excitations in the heat bath outside the core. If  $\omega_0\tau < 1$  the levels overlap and spectral flow is allowed. This type of spectral flow is analogous to “hopping conduction” in a solid; it is assisted rather than impeded by collisions.

(b) Such spectral flow is induced by the motion of the vortex with respect to the heat bath. If the vortex moves with velocity  $v_x$  along  $x$  the rate of change of excitation angular momentum in the moving core is  $\dot{L}_z = \dot{x}p_y = v_x p_y$ . The levels cross zero at a rate  $-\dot{L}_z/\hbar$  leading to spectral flow in opposite senses for  $p_y > 0$  and  $p_y < 0$  as indicated. Since the left-handed quasiparticles created for  $p_y > 0$  are equal in number to the right-handed quasiholes created for  $p_y < 0$  there is no net production of chiral charge  $C$ , but excitation momentum is created at a rate  $\dot{p}_y = -v_x p_y^2/\hbar$ , independent of the sign of  $p_y$  (shown for negative  $v_x$ ).

(c) An example of an  $N = 2$  continuous vortex in  $^3\text{He-A}$ . The cones indicate the local direction of the order parameter vector  $\hat{\mathbf{l}}$ , which is parallel to the angular momentum of the Cooper pairs, and is analogous to the direction of the isotopic spin in electroweak theory. Rotation of the cones about  $\hat{\mathbf{l}}$  indicates a change in phase of the order parameter; note the  $4\pi$  phase change around the perimeter of the diagram, corresponding to two quanta of anticlockwise circulation. Four topologically different types of  $^3\text{He-A}$  vortices have been observed [23].

Fig. 3: (a) *Upper inset* Experimental cell. The aluminized Kapton film diaphragm separates two disc-shaped regions of superfluid  $^3\text{He}$ , each  $100\mu\text{m}$  thick. The roof of the cell has six electrodes set into it by means of which the oscillations of the diaphragm may be driven and detected electrostatically. In the oscillating modes of interest the motion of the diaphragm displaces the superfluid as indicated, while the normal component of the fluid (the heat bath) is clamped by its high viscosity. Rotation at angular velocity  $\Omega$  about a vertical axis produces vortices normal to the diaphragm. These vortices produce additional dissipation proportional to  $\alpha\Omega$  and coupling between two orthogonal modes of the diaphragm, with displacement patterns shown in the *lower inset*, proportional to  $(1 - \alpha')\Omega$ . The measured

spectral flow parameters are related to the parameters in Ref. [20] by  $\alpha = B\rho_n/2\rho$  and  $\alpha' = B'\rho_n/2\rho$ .

*Main frame* The measured  $(1 - \alpha')/\alpha$  for  $^3\text{He-B}$  at 20bar is compared with the theoretical value  $(1 - \alpha')/\alpha \approx \omega_0\tau$ . The temperature dependence of  $\omega_0\tau$  is not very well known, since it is sensitive to the details of the quasiparticle scattering. It can be estimated by the formula  $\omega_0\tau = (a\Delta(T)/k_B T)^2 \exp(\Delta(T)/k_B T)$  [19]. The solid line is for  $a = 0.067$ . The fit is much improved if an effective energy gap 0.6 of the bulk value is assumed; the dashed line is for  $\Delta(T) = 0.6\Delta_{\text{bulk}}(T)$  and  $a = 0.214$ . But the justification for such an assumption is not clear.

(b) The experimental parameter  $(1 - \alpha')$  for  $^3\text{He-B}$  at 20bar is compared with the ‘spectral flow’ prediction of Eq. (5):  $(1 - \alpha') \approx n_s(T)/(n \tanh(\Delta(T)/2k_B T))$  (solid line). Note that this fit is independent of the relaxation parameter  $\omega_0\tau$ . The dashed line is for  $\Delta(T) = 0.6\Delta_{\text{bulk}}(T)$ , and fits much better below  $0.6T_c$ . This fit shows that spectral flow is less strongly suppressed at low temperatures than the full energy gap would suggest.

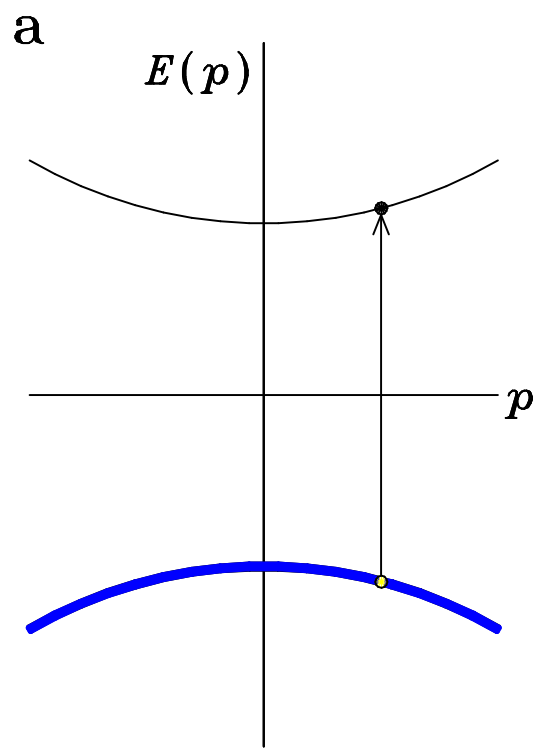


Figure 1(a)

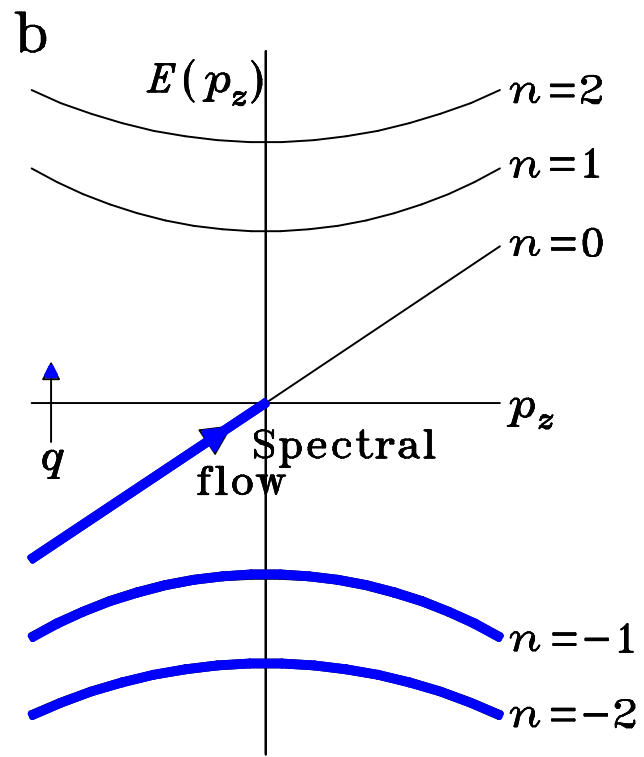


Figure 1(b)

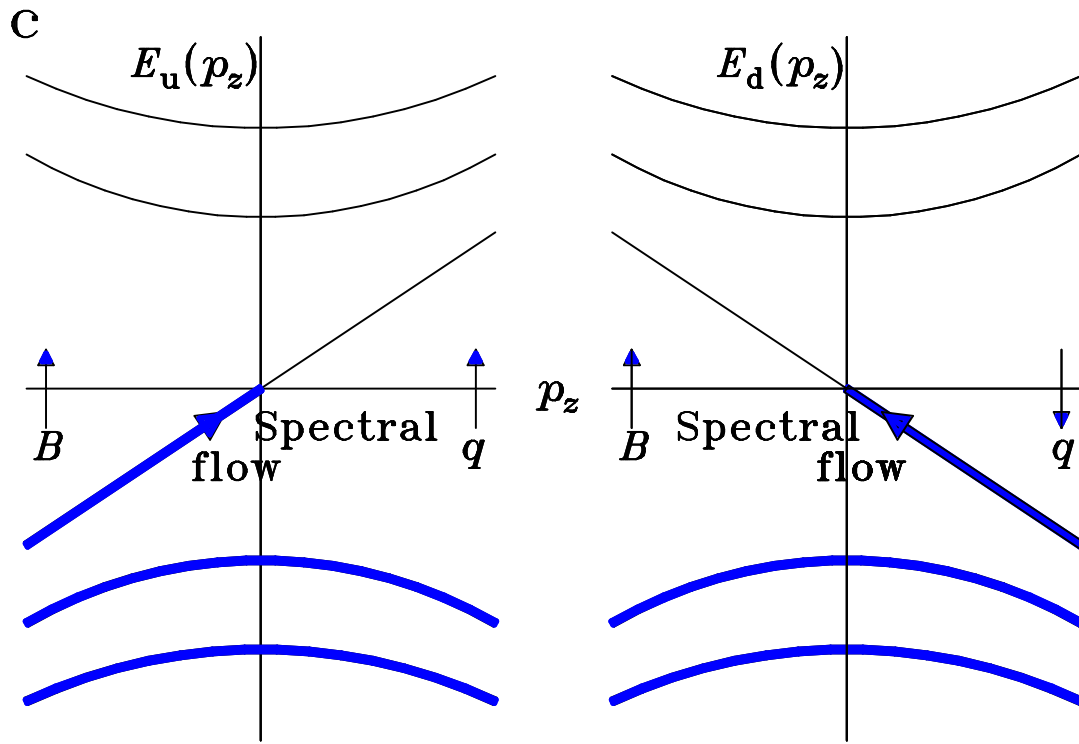


Figure 1(c)

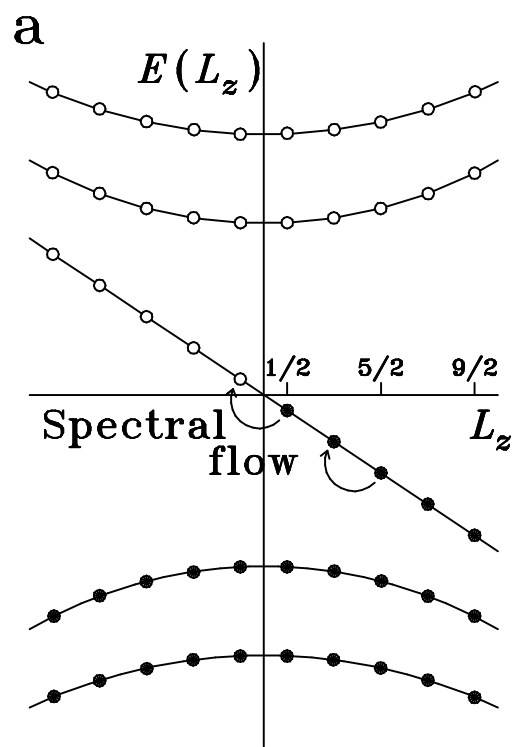


Figure 2(a)



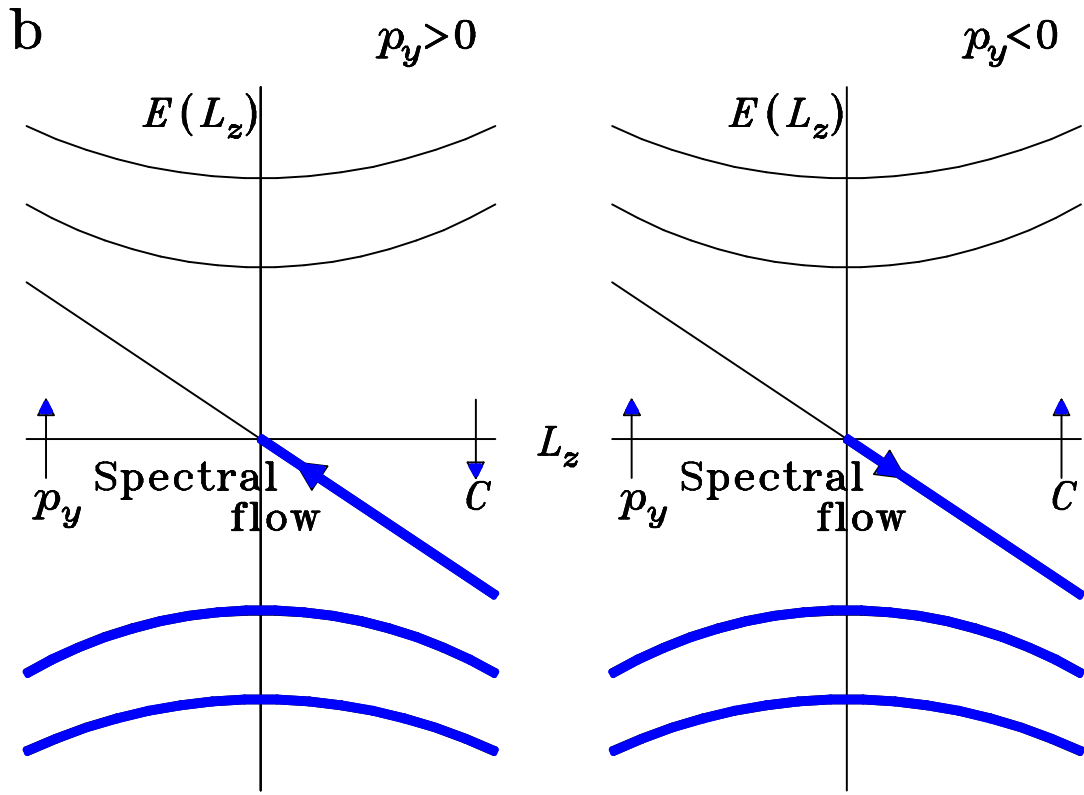


Figure 2(b)

c

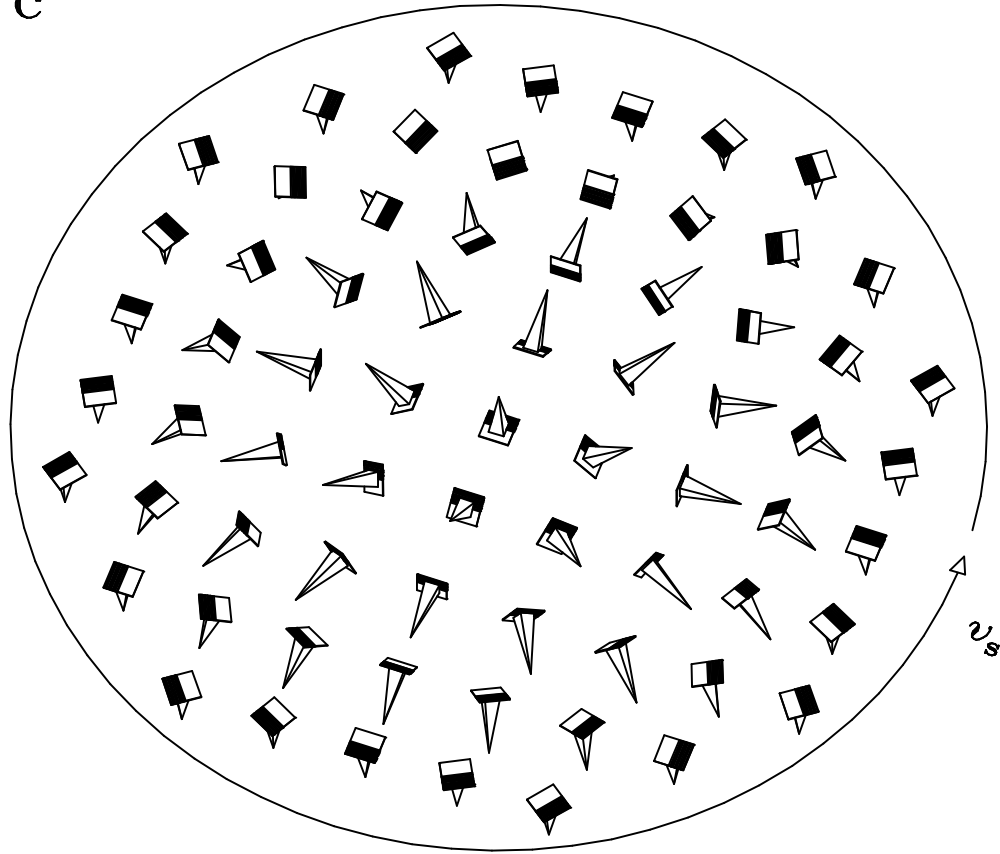


Figure 2(c)

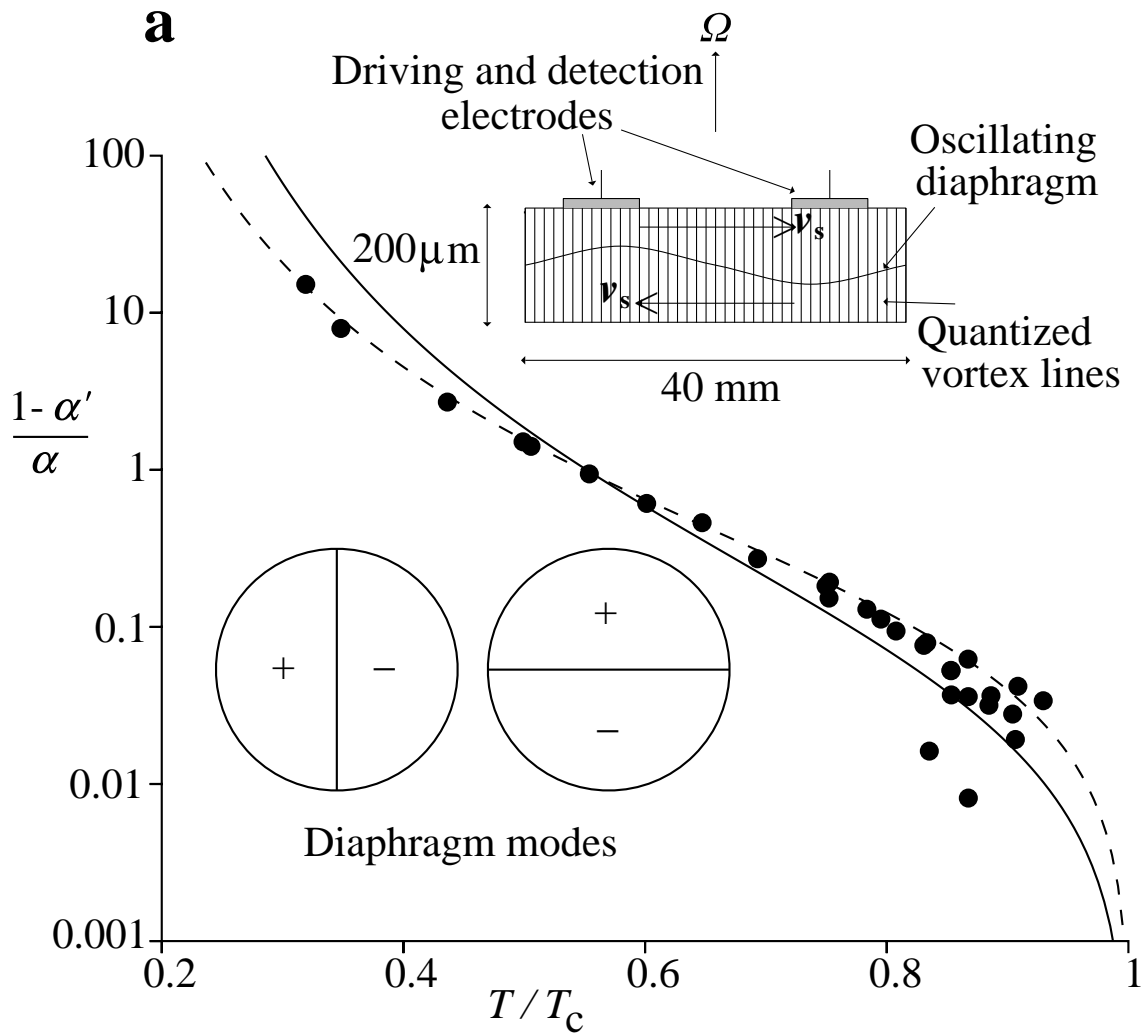


Figure 3(a)

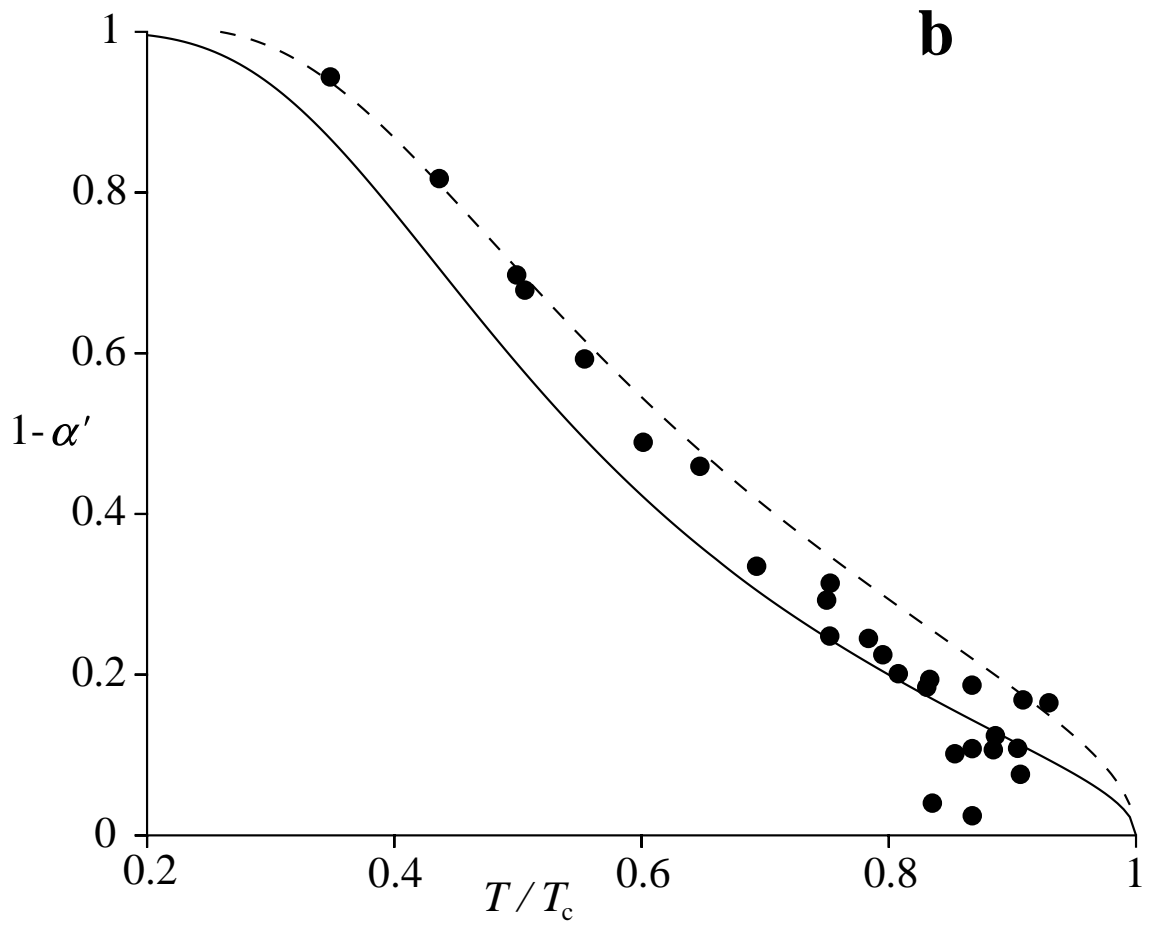


Figure 3(b)